Optimal acquisition parameters for smart DAS uphole survey in a desert environment

Ezzedeen Alfataierge, Moneera Alsharif, Andrey Bakulin, EXPEC Advanced Research Center, Saudi Aramco; and Anton Egorov, Aramco Research Center – Moscow, Aramco Innovations LLC*

SUMMARY

We conduct detailed modeling and evaluation of a smart DAS uphole survey that uses Distributed Acoustic Sensing (DAS) with cemented fiber. We simulate DAS and geophone surveys in a deep 300 m uphole. We use a realistic elastic near-surface model typical for a complex desert environment. The time-depth curves extracted from the simulated DAS and geophone records produce comparable results. We further analyze the effect of DAS acquisition parameters and source offset on traveltimes and inverted velocities. We show the importance of using a small gauge length of 1-2 m for accurate characterization of the shallowest 50 m. Likewise, the smallest source offset should be used for this section. In the deeper portion of the survey, below 50 m depth, larger gauge length and the source offset become acceptable. A DAS survey with a moderate GL of 6 m allows accurate delineation of alternating thin high and low-velocity layers important for the robust model building of higher-resolution initial models.

INTRODUCTION

Near-surface velocity model building remains critical for the success of seismic imaging, particularly in the desert environment. Topography, extremely low velocities, and alternating highly contrasting layers create challenges for seismic imaging. Simultaneously, surface seismic surveys are designed for deep targets and often lack the necessary density to characterize the near surface reliably. Even if imaging of deeper targets is acceptable, errors in a long-wavelength spatial component of near-surface velocity may result in false structures or distortion of real ones (Ley et al., 2003; Bakulin et al., 2017). Seismic upholes play a critical role in describing complex near surface (Cox, 1999). In a desert environment, uphole-based models such as single-layer and multi-layer models have long played an essential role in de-risking and imaging low-relief structures (Ley et l., 2003; Bridle et al., 2003). Refraction tomography and then full-waveform inversion has become popular and widespread. All of these methods need good initial models as well as accurate calibration. Indeed, it is unthinkable to perform reliable depth imaging of deep targets without using velocity calibration from existing wells. Near-surface model building is, in essence, a mini-depth imaging problem. Uphole surveys (Cox, 1999) play the role of "shallow wells" needed to achieve similar calibration. Egorov et al. (2020) have shown that refraction tomography with surface data carries significant uncertainty. Adding uphole data can lead to a reduction in this uncertainty to a level acceptable for low-relief structures. Al-Abri (2021) demonstrated a critical role of borehole near-surface velocities to construct initial models for FWI.

Conventional uphole surveys are conducted with a single-geophone tool slowly raised from the bottom to the top of the well (Cox, 1999). Such surveys are time-consuming and risky since the hole may collapse at any moment in time. Besides, variable source wavelets and receiver couplings for each recording and imperfect depth control may further reduce the quality of the results. Bakulin et al. (2017) proposed smart DAS (Distributed Acoustic Sensing) upholes that utilize preinstalled fiber-optic cables. They can be acquired with a single shot resulting in consistent wavelets and delivering dense, high-quality data. Smart DAS upholes open many additional opportunities from the quick acquisition of walkaway uphole surveys to amplitude-based DAS logging to attenuation estimation to repeating measurement with time (if the cable is permanently installed).

This study focuses on elastic finite-difference modeling of a smart DAS uphole survey using a realistic model of the arid near surface shown in Figure 1. We focus on accurate extraction of near-surface velocity profiles using first-break traveltimes. Specifically, we investigate the influence of various DAS acquisition parameters and compare results with conventional uphole surveys with geophones.

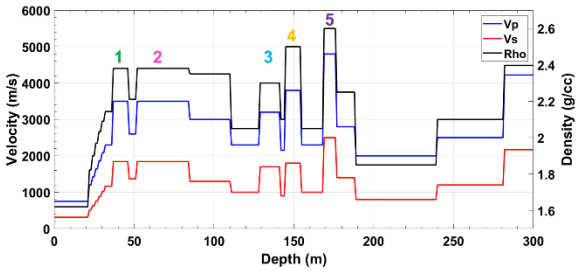

Figure 1: Realistic near-surface model from the desert environment. Observe alternating high- and low-velocity layers with extreme velocity contrasts reaching 200%. High-velocity layers 1-5 are highlighted for later reference in the analysis.

MODELING APPROACH

For simulation, we employ a realistic modeling approach that uses a modeling code based on a 2D pseudospectral elastic method (Fornberg, 1987). DAS cable directivity and the gauge length effects are accurately modeled by transforming numerically computed point strains into distributed responses measured by the DAS sensor.

DOI:10.1190/segam2021-3567899.1

NEAR-SURFACE MODEL FROM DESERT ENVIRONMENT

The near-surface model (Figure 1) is inspired by one of the actual onshore fields (Alexandrov et al., 2015). It has many typical characteristics features of shallow subsurface in a desert environment. The first layer of sand has constant properties with a longitudinal velocity of 750 m/s, which is a significant oversimplification (Robinson and Al-Husseini, 1982; Bridle, 2017). The rapid gradient of velocities occurs below the sand layer down to 40 m. Two high-velocity layers are present at 37 and 52 m underlain by lower velocity strata. Such high-velocity layers can act as a "screen" and profoundly affect refracted and reflected energy (Poley and Nooteboom, 1966). The deeper part (80-300 m) contains several additional alternations of high- and low-velocity layers with velocity contrasts reaching as high a 200%. A free surface is used on the top of the model.

ACQUISITION GEOMETRY AND MODELING

We consider a smart DAS uphole with the depth of 300 m required to characterize the near-surface complexity above. Such characterization cannot be achieved with borehole geophysics surveys in deep wells due to the presence of three and more strings of casing in this interval. Since DAS provides uncompromised sampling, we evaluate several survey geometries with one-meter receiver sampling, an improvement over variable 2-6 m spacing used in geophone uphole. We consider four source offsets. The Fuchs-Müller (minimum phase) wavelet with 45 Hz central frequency is used as the modeling source. The critical acquisition parameter for DAS acquisition is the so-called gauge length (GL) – the length of the fiber delivering single trace output. The GL acts as a linear seismic array and should be carefully chosen, striking a balance between capturing the lowest velocities in the subsurface while maintaining a good signal-to-noise ratio (Bakulin et al., 2020). Therefore, for each source offset, we evaluate several acquisition scenarios with different GLs described in Table 1.

Source Depth			**Receiver Depth**			**Spatial Sampling**	
0 m			0-300 m			1 m	
Time Sampling	**Record Length**		**Source Type**			**Source Frequency**	
0.5 ms	300 ms		Fuchs-Muller			45 Hz	
Source Offset	**Gauge Length (m)**						
0	2	4	6	8	10	15	20
5	2	4	6	8	10	15	20
10	2	4	6	8	10	15	20
15	2	4	5	8	10	15	20

Table 1. Acquisition and modeling parameters.

This study serves as feasibility for future field data acquisition. Therefore, we performed full-waveform modeling that fully accounts for DAS's directivity and gauge length effects (Figure 2). Data analysis in this study focuses on traveltimes and velocity derived from traveltimes, whereas other studies would analyze amplitude response and waveform usage. First breaks were picked using an automated picker. First excursion (peak or trough) was followed accordingly for each of the particle velocity (geophone uphole measurement) and DAS strain records (smart DAS uphole).

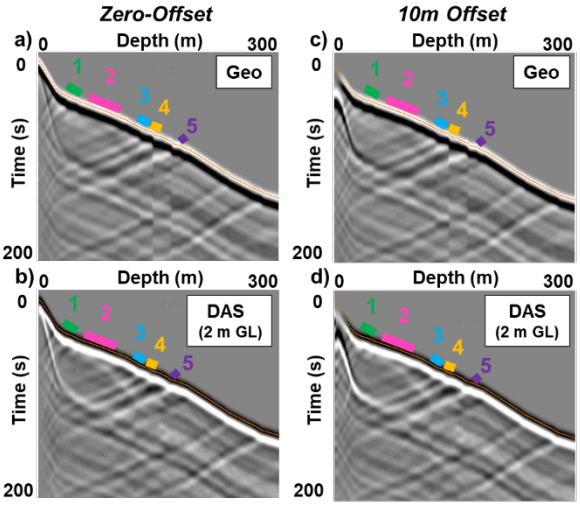

Figure 2: Zero-offset synthetic gathers of particle velocity (a) and DAS strain with 2 m GL (b), overlaid with first break picks (orange). Likewise, (c) and (e) display similar results for 10 m source offset. Gathers have RMS amplitude scaling applied. Positions of high-velocity layers 1-5 are shown colored segments above the first breaks.

Figures 2a and 2b show continuous first arrivals from the shallowest depth and sharp reflections at the contrasting interfaces clearly visible without wave separation. In contrast, offset gathers on Figures 2c and 2d show loss of continuity of the first break event at a shallow depth consistent with the source offset. Therefore, manual picks were done to override the automatic picker at these depths and attempt deriving picks as close to the surface as possible. The traveltimes were then shifted by a quarter of the period (T/4) to approximate the onset or first breaks. Figure 3 shows derived traveltimes from geophone and three DAS acquisition geometries.

Figure 3a shows traveltime picks obtained from geophone and DAS data when the source is at zero offset. Figure 3b verifies that the bulk of the traveltimes are within ~ 1 ms from the modeled times. More significant deviations are seen in the first 50 m, particularly for DAS with GL of 15 m.

Like a disproportionately large geophone array can distort the signal, large GL can also be damaging, particularly when near-surface velocities are low. GL of 15 m appears perfectly acceptable for velocity estimation below 50 m (Figure 3). A larger GL of 30-50 m is routinely for deep 3D VSP imaging in deep water. However, we must use small gauge lengths to derive reliable velocities in the shallow sections for near-surface problems. Considering that *P*-wave velocity in the sand can be significantly lower than 750 m/s used in this model - the smallest possible GL with acceptable SNR is preferred.

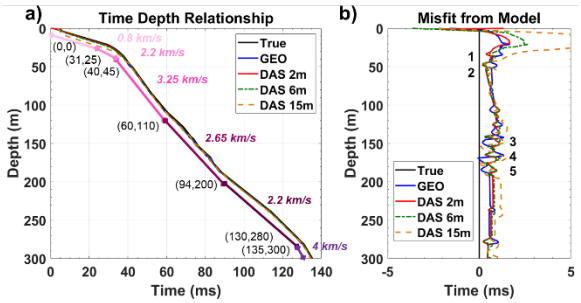

Figure 3: (a) Time-depth curves obtained from geophone data (particle velocity, blue) and DAS with GL = 2m (red), 6m (green), and 15m (orange). For reference, time-depth computed by slowness integration of the true vertical profile is shown in black. Manual uphole interpretation (Cox, 1999) is annotated for six layers (pink-purple). (b) Same as (a) but shown as a difference between picked and true model traveltimes. Data from zero-offset source is used here.

VELOCITY ESTIMATION AND EFFECT OF ACQUISITION PARAMETERS

The time-depth curve may be inverted for interval velocities. As expected, non-regularized inversion dividing the receiver spacing by the change in traveltime (Figure 4, dotted lines), results in large velocity fluctuations even for noise-free synthetic data. This is caused by errors in traveltimes extracted from finite-frequency data. In contrast, regularized inversion using the method from Lizarralde and Swift (1999) delivers more robust results (Figure 4, solid lines). Inversion minimizes traveltime differences between predicted and picked traveltimes in the least-squares sense. However, an additional regularization term in the objective function leads to a velocity model with a certain level of smoothness controlled by the regularization parameter. Such regularization suppresses spurious velocity fluctuations while recovers a smoother version of interval velocity that explains observed traveltimes. Figure 5 shows final residuals vs. depth. The average traveltime error is well below 1 ms. The errors are not accumulating with depth as in other simple inversion approaches.

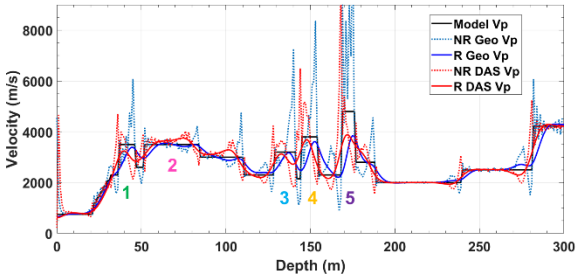

Figure 4: Comparison between regularized (solid) and nonregularized (dotted) inverted interval velocities from geophone (blue) and DAS with 2 m GL (red) data w.r.t. zero-offset source. True velocity is shown in black, and high-velocity layers 1-5 are labeled.

While regularized inversion cannot accurately delineate the high-contrast boundaries, it reliably identifies all five high-velocity layers (Figure 4). The decimation of receiver spacing (2 m, 5 m) leads to an even smoother velocity profile with reduced vertical resolution. This confirms that using small spacing on the order of 1 m with DAS should enable the best resolution to delineate thin high-velocity layers. Insertion of such contrasting layers into the initial model could be beneficial for successful FWI in a desert environment (Al-Abri, 2021). While smoothed sonic logs can deliver this information, they are rarely available for such shallow depth. We demonstrate here that such delineation can be achieved with smart DAS uphole surveys.

Elevated errors in the first 5 m (Figure 5) indicate that inversion is unable to find any model that could satisfy picked traveltimes. Figure 3b verifies that those picked traveltimes deviate significantly from the modeled ones. We speculate that picked traveltimes in the near-field zone are likely distorted. Unlike the far zone, where traveltime inversion is perfectly stable, the near zone is complicated by a complex near field with variable wavelets. Usage of waveform-based methods may account for near-field effects and a better estimate of the near-surface's topmost layer.

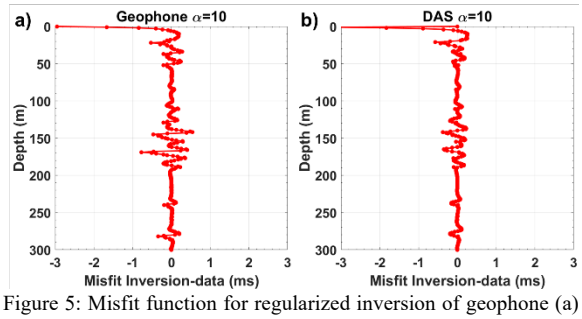

Figure 5: Misfit function for regularized inversion of geophone (a) and DAS (b) data with GL=2 m.

DOI:10.1190/segam2021-3567899.1

Regularized inversion for three different GL of 2, 6, and 15 m are shown in Figure 6. There are minimal differences between 2 m and 6 m curves. Smaller GL results in a somewhat higher velocity closer to real values inside high-velocity layers 1-5. In contrast, 16 m GL results in a profile with much less vertical resolution even at deeper depths of 100-300 m. Most acute differences are seen in the first 50 m interval. Orange curve completely misses the first high-velocity layer. Besides, it results in an artificial hump between 0 and 15 m, distorted shallow traveltimes. Such shallow distortion at large GL may be caused by the interaction of DAS array averaging, near-field effects, as well as edge effects of DAS acquisition. If we examine misfit functions for these three cases, they all exhibit similar behavior with average errors below 1 ms.

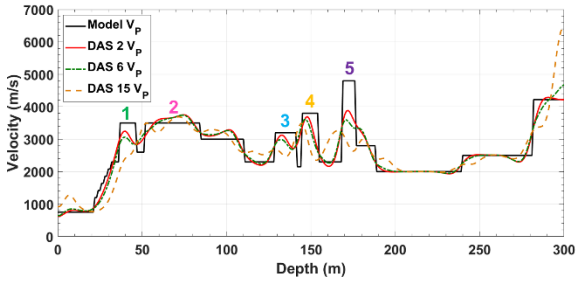

Figure 6: Regularized inversion for interval velocity profile using DAS surveys with different gauge lengths: 2 m GL (blue), 6 m GL (orange), and 15 m GL (yellow). True velocity is shown in black.

Additionally, we observe opposite patterns of traveltime residuals between the geophone and DAS at layer boundaries (Figure 3b). These fluctuations can be explained by the opposite polarity of downgoing waves on DAS and geophone gathers, whereas they have the same polarity for upgoing waves (Mateeva et al., 2014). Different interference patterns for DAS and geophone data explain different signs of these small fluctuations. It should be noted that these fluctuations occur only at highly contrasting boundaries and are not observed for smooth velocity profiles. This gives additional impetus for using waveform-based methods to characterize the highly-contrasting near-surface layers in a desert environment.

Consistent with field observation (Bakulin et al., 2018) in the shallow sections with the slowest velocities, we similarly find that the increase in GL leads to the broadening of the first break wavelet, suggesting filtering of higher frequencies by DAS array. Finally, we examine the effect of the source offset (Figure 7). The effect of source offset is minimal on velocities below 60 m. However, 1st and 2nd layers become less resolved with GL of 2 m and 6 m, indicating a loss of accuracy. As for GL of 15 m, the shallow section (0-60 m) exhibits larger variations than seen in Figure 6, again suggesting more adverse effects in the shallow section.

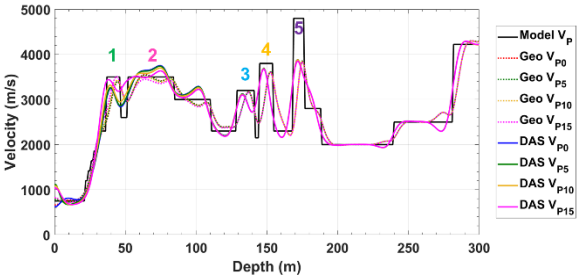

Figure 7: Regularized inversion interval velocity for geophone (dashed) and DAS 2 m GL (solid) at different source offsets (0, 5, 10, and 15 m). All traveltimes are shown after verticalization (Cox, 1999).

CONCLUSIONS

We have presented realistic modeling of smart DAS uphole survey in a complex near-surface model from a desert environment. We confirmed that the DAS survey produces comparable time-depth curves to conventional geophone uphole surveying. The higher density of DAS acquisition assists with reliably resolving alternating high and low-velocity layers present in the shallow subsurface. Impact of DAS acquisition parameters and offset on the resulting velocity is minimal below 50 m depth. For the best delineation of shallowest layers with slowest velocities, a small gauge length should be selected. Gauge length is assigned in the interrogator, and DAS uphole can be acquired with a single shot. As a result, both small (1-2 m) and large (4-8 m) GL records can be acquired simultaneously in practice. Small gauge length would allow the highest resolution at a shallower depth, while larger GL gives the best signal-to-noise for deeper recording. Using a smaller offset is recommended for the first 50 m. If a smart DAS uphole uses fiber cemented in place, then such acquisition becomes possible. We further observed complex waveform interference of downgoing and upgoing waves at high-contrast interfaces. We conclude that waveform-based methods may further improve vertical resolution of inverted velocity profiles compared to traveltime inversion of even densely-sampled uphole surveys with DAS.

REFERENCES

Al-Abri, S., 2021, Field focused velocity model building in PDO: Tips and Pitfalls: SEG/DGS Workshop on Challenges and New Advances in Velocity Model Building.

Alexandrov, D., A. Bakulin, R. Burnstad, and B. Kashtan, 2015, Improving imaging and repeatability on land using virtual source redatuming with shallow buried receivers: Geophysics, **80**, no. 2, Q15–Q26, doi: https://doi.org/10.1190/geo2014-0373.1.

Bakulin, A., P. Golikov, E. Erickson, I. Silvestrov, Y. S. Kim, R. Smith, and M. Al-Ali, 2018, Smart DAS uphole acquisition system for near-surface characterization and imaging: 88th Annual International Meeting, SEG, Expanded Abstracts, 16–20, doi: https://doi.org/10.1190/segam2018-2995883.1.

Bakulin, A., P. Golikov, R. Smith, E. Erickson, I. Silvestrov, and M. Al-Ali, 2017, Smart DAS upholes for simultaneous land near-surface characterization and subsurface imaging: The Leading Edge, **36**, 1001–1008, doi: https://doi.org/10.1190/tle36121001.1.

Bakulin, A., I. Silvestrov, and R. Pevzner, 2020, Surface seismic with DAS: An emerging alternative to modern point- sensor acquisitions: The Leading Edge, **39**, 808–818, doi: https://doi.org/10.1190/tle39110808.1.

Bridle, R., 2017, Sand curve facelift: Empirical to polynomial model and the effect on the tomogram: Geophysics, **82**, no. 3, U37–U48, doi: https://doi.org/10.1190/geo2016-0175.1.

Bridle, R., R. Ley, M. Al-Homaili, M. Maddison, and K. Janssen, 2003, Practical application of implementing a layer model with control from first breaks in Saudi Arabia: SEG Technical Program, Expanded Abstracts, 1996–1999, doi: https://doi.org/10.1190/1.1817719.

Cox, M., 1999, Static corrections for seismic reflection surveys: SEG, 546.

Egorov, A., P. Golikov, I. Silvestrov, and A. Bakulin, 2020, Near-surface velocity uncertainty estimation through Bayesian tomography approach: SEG International Exposition and 90th Annual Meeting, 3634–3638, doi: https://doi.org/10.1190/segam2020-3411920.1.

Fornberg, B., 1987, The pseudospectral method: Comparisons with finite differences for the elastic wave equation: Geophysics, **52**, 483–501, doi: https://doi.org/10.1190/1.1442319.

Ley, R., R. Bridle, D. Amarasinghe, M. Al-Homaili, M. Al-Ali, M. Zinger, and W. Rowe, 2003, Development of near surface models in Saudi Arabia for low relief structures and complex near surface geology: SEG Technical Program, Expanded Abstracts, 1992–1995, doi: https://doi.org/10.1190/1.1817718.

Lizarralde, D., and S. Swift, 1999, Smooth inversion of VSP traveltime data: Geophysics, **64**, 659–661, doi: https://doi.org/10.1190/1.1444574.

Mateeva, A., J. Lopez, H. Potters, J. Mestayer, B. Cox, D. Kiyashchenko, P. Wills, S. Grandi, K. Hornman, B. Kuvshinov, W. Berlang, S. Yang, and R. Detomo, 2014, Distributed acoustic sensing for reservoir monitoring with vertical seismic profiling: Geophysical Prospecting, **62**, 679–692, doi: https://doi.org/10.1111/1365-2478.12116.

Poley, J. P., and J. J. Nooteboom, 1966, Seismic refraction and screening by thin high-velocity layers (A scaled model study): Geophysical Prospecting, **14**, 184–203, doi: https://doi.org/10.1111/j.1365-2478.1966.tb01754.x.

Robinson, D. K., and M. Al-Husseini, 1982, Technique for reflection prospecting in the Rub' Al-Khali: Geophysics, **47**, 1135–1152, doi: https://doi.org/10.1190/1.1441377.